THE ASTROPHYSICAL JOURNAL, 435:L15–L18, 1994 November 1

HST/FOC IMAGING OF THE NARROW-LINE REGION OF NGC 1068[1]

F. MACCHETTO,[2,3] A. CAPETTI,[2] W. B. SPARKS,[2] D. J. AXON,[2,3] AND A. BOKSENBERG[4]

Received 1994 May 17; accepted 1994 August 11

ABSTRACT

We present imaging observations of NGC 1068 taken with the COSTAR-corrected (Corrective-Optics Space Telescope Axial Replacement) Faint Object Camera on board the *Hubble Space Telescope* in the UV and optical continuum and [O III] emission lines. From these observations the structure of the nuclear region of NGC 1068 is shown to be very complex. Bright filamentary and patchy structures are intermingled with dark lanes. Other interesting features are identified, including the location of the UV peak with respect to the peak of line emission, the existence of an unusual "twin-crescent" object near the nucleus, and point sources in the field. In the UV to optical flux ratio image, an extended conical region stands out for its blue color which may be tracing reflected nuclear light.

Subject headings: galaxies: Seyfert — galaxies: individual (NGC 1068)

1. INTRODUCTION

When the *Hubble Space Telescope* (*HST*) was first launched one of the key areas in which its diffraction-limited resolution was expected to revolutionize our understanding was in the physical structure and origin of the narrow-line region (NLR) of active galactic nuclei (AGNs). NGC 1068 is the nearest classical Seyfert 2 and the first in which it was recognized that in polarized light some narrow-line AGNs show the broad permitted lines which characterize a Type I Seyfert galaxy (Antonucci & Miller 1985). Comprehensive ground-based studies have shown that its NLR is cospatial with a complex linear radio source $\sim 7''$ in extent (Wilson & Ulvestad 1983) and displays the kinematic hallmarks of expansion driven by interaction with the ejected radio plasma (Meaburn & Pedlar 1986; Baldwin, Wilson, & Whittle 1987). At larger radii, emission-line spectroscopy and imaging reveal that as with other Seyfert galaxies with linear radio sources (Unger et al. 1987), NGC 1068 has an extended narrow-line region (ENLR) whose axis is aligned with that of the radio source. Both the ENLR (Unger et al. 1992) and the NLR (Pogge 1989) share a roughly conical shape, indicative of photoionization by a collimated nuclear radiation field, reinforcing the idea that the nucleus is shrouded in a dense molecular torus whose polar axis is inclined at a large angle to our line of sight.

Optical imaging observations of the NLR obtained with WF/PC1 and the aberrated *HST* were presented by Evans et al. (1991) and revealed the presence of several distinct clouds in the NLR. Here, for the first time, we present diffraction limited high dynamic range Faint Object Camera (FOC)/Corrective Optics Space Telescope Axial Replacement (COSTAR) images of the NLR of NGC 1068 obtained after the *HST* refurbishment mission. These images, taken in UV continuum, blue optical continuum and [O III] line emission, reveal the remarkable complexity of the hitherto unseen structure of the NLR and show the potential of *HST* for advancing our physical understanding of AGNs.

We assume the distance of NGC 1068 to be 22.7 Mpc, and thus $0''.1$ corresponds to 11 pc.

2. OBSERVATIONS AND DATA REDUCTION

NGC 1068 was observed using the FOC on board the *Hubble Space Telescope*, after the COSTAR deployment. The observations were taken in 1994 January 10, in the f/96, 512×512 mode (Paresce 1992) which with the COSTAR corrective optics becomes f/151 (Jedrzejewski et al., 1994); the pixel size is $0''.014 \times 0''.014$ and the field of view $\sim 7'' \times 7''$. We used two medium-band filters (F253M and F372M) and one narrow-band filter (F501N). Filters F372M and F501N were also used in combination with the neutral density F4ND. The exposure time for each observation was 1200 s. The F372M transmission curve is similar to a standard U filter and hereafter, for convenience, it will be referred to as the U' filter. Data were processed to correct for geometric distortion and flat-field response in the standard manner. Resau marks were removed from the images by interpolation and a flat-field linearity correction was applied.

In some regions, the U' and [O III] images exceed the maximum count rate and therefore are nonlinear or even saturated. To correct for this effect, the nonlinear portions of the images were filled with appropriately scaled portions of images taken with the neutral density filters F4ND (the scaling factor was found empirically to be 3.85 mag). This extends the dynamic range (peak to rms noise) to ≈ 3000 at both wavelengths. In the UV image the count rate never exceeds 0.8 counts s^{-1} and only exceeds 0.5 counts s^{-1} in one very small region; thus residual errors after the linearity correction are expected to be smaller than a few percent. Nonlinearity in FOC images is associated with a low-level pattern noise (less than 10%) which was removed by Fourier filtering. Spatial registration of the images was performed using point sources in the frame. The FWHM of these sources was measured to be $0''.025$ in the UV and $0''.050$ in the optical, consistent with the diffraction-limited performance of the refurbished *HST*.

3. RESULTS

Many emission lines are present in the wavelength range covered by the F253M and F372M filters. The contribution of

[1] Based on observations with the NASA/ESA *Hubble Space Telescope*, obtained at the Space Telescope Science Institute, which is operated by AURA, Inc., under NASA contract NAS 5-26555.

[2] Space Telescope Science Institute; 3700 San Martin Drive, Baltimore, MD 21218.

[3] Astrophysics Division, Space Science Department of ESA; ESTEC, NL-2200 AG Noordwijk, The Netherlands.

[4] Royal Greenwich Observatory; Madingley Road, Cambridge CB3 0EZ, UK.

these lines to the total counts depends on the exact aperture size and location; using archival FOS spectra taken with different pointings and aperture sizes, we infer ~5%–10% for the F253M and ~15%–20% for the F372M filter. On the other hand, F501N is well centered on [O III] λλ4959, 5007 which produce more than 90% of the total counts. Thus, the two medium-band images (Figs. 1*a*–1*b* [Pl. L4]) show essentially continuum emission while the narrow-band filter gives an [O III] emission-line image (Fig. 1*c* [Pl. L4]). Using synthetic photometry with archival pre-COSTAR FOS data, we estimate that emission longward of 3000 Å contributes less than 0.5% in the F253M filter: i.e., there is no significant red leak in the UV image. Figures 1*a*–1*c* show the final images for each filter separately. Figure 1*d* (Plate L4) shows a summed image, all three wavelengths, shown at high contrast. Figure 2 (Plate L5) is a color composite in which the *U′* is assigned to "red," UV continuum to "blue" and the [O III] line emission image to "green." This rendering is dominated by the differences between the *U′* continuum and [O III] emission. Figure 3*a* and 3*b* (Plate L6) show an expanded version of the central region of the UV continuum and oxygen emission-line images, respectively.

The initial impression is that images at all three wavelengths are very similar; however, they differ in detail. They contain a complex structure, with bright filaments and patches intermingled with dark lanes. We refer to the brightest feature in the images as cloud B, following Evans et al. (1991). This region is well resolved in the new data, and its morphology and color are discussed in detail in § 3.2. It lies at the apex of a bright "conelike" structure, familiar from the earlier data of Evans et al. (1991). At higher contrast, Figure 1*d*, we also see a "cone" morphology; however, the location of the apex is further south and the axis of symmetry is rotated clockwise from the previous one. This change in orientation of the inner cone is shown in more detail in Figure 3*a*. This is reminiscent of the situation with the very large scale ionized gas distribution, where Unger et al. (1992) show a sharp conical structure oriented some 30° counterclockwise from these inner cones. The color composite image, Figure 2, shows that the *U′* continuum envelopes the [O III] emission region, and may delineate the true boundaries of the cone.

If there is in fact a wide angle cone, then the changing cone P.A. with distance from the nucleus may be due to the different location of the gas as it streams around the inner bar of NGC 1068, and intersects the cone at a changing angle. The radio emission shows a similar bending, which may also be due to pressure gradients associated with the gas motions, or else it may be that the ionization and scattering cone is indeed fairly narrow and tracks the radio jet more closely, perhaps due to precession effects or to different sources of radiation.

In addition to the conical structures of the northern filament complex, there is substantial emission to the south of the nucleus. This is less extensive, and consistent with a counterjet or cone region seen through the galactic disk; see § 3.1.

Toward the top of each image, the morphology becomes more filamentary, with arcs sweeping around and toward the nucleus in the same sense as the large-scale spiral structure of NGC 1068. There are in addition some individual features of interest; 0.″6 south (P.A. +163°) of the emission peak is a ring-like or double-jet–like feature which will be referred to as the "twin-crescent" structure. This is isolated and shown in Figures 3*c* and 3*d* and discussed in § 3.3. In this region, which is close to the nucleus of NGC 1068, there are also straight rays, visible in Figure 1*d* and perhaps best seen in Figure 2. These rays are seen in both optical wavebands images. Those emerging on the left side are narrow and sharp edged, while those emerging on the right side are more diffuse. These are reminiscent of the features seen in the equatorial plane of η Carinae (Hester et al. 1994), albeit here at much lower S/N. Finally, there are a number of individual unresolved sources in the field, Figure 1*d*, whose colors and luminosities are discussed in § 3.4.

3.1. *UV-Optical Color Image*

Figure 4 (Plate L7) shows the ratio between the UV and *U′* continuum images; lighter colors correspond to a bluer spectrum. The nuclear region has a bluer color with respect to the underlying galaxy; this bluer region extends for more than 4″ and describes a conical structure. The color is quite uniform over this region with the ratio between UV and *U′* fluxes (both in units of ergs s^{-1} cm^{-2} $Å^{-1}$) being between 1.1 and 1.5. Close to the nucleus, there is correlation between color and surface brightness in the sense that the colors become bluer as the brightness increases. For example, on the emission peak (cloud B) the UV flux is 1.7 times the *U′* flux; this ratio is in good agreement with the archival FOS observations through the 0.″3 aperture. The bright structures toward the south also have very blue colors, although not as blue as on the north side: characteristically $F_{UV}/F_{opt} \sim 0.75$.

Spectropolarimetric observations suggest that light from a hidden nucleus is reflected into our line of sight (Antonucci & Miller 1985); the anisotropy of the nuclear emission of NGC 1068 is confirmed by the discovery of extended ionization cones (Pogge et al. 1989). In this framework, the conical blue region observed in Figure 4*a* is where the scattering of the intrinsically blue nuclear light is occurring.

The northern emission-line region is thought to lie above the plane of the galaxy (Unger et al. 1992) so that the southern region is seen through the galaxy disk. The asymmetry between the north and south regions of emission lines can be ascribed to the reddening in the host galaxy. Using the reddening curves of Cardelli, Clayton, & Mathis (1989) this color difference corresponds to an absorption excess in the south lobe of $\Delta E(B-V) = 0.25 \pm 0.05$ with respect to the north lobe. The column density derived from the standard dust-to-gas ratio is 2×10^{21} cm^{-2}, consistent with typical Galactic values. This estimate indicates that the disk is not optically thick, in agreement with IR imaging polarimetry (J. J. Hough, private communication) which shows the counterlobe in polarized light.

3.2. *Structure of Cloud B*

Much of the interest in the structure of the emission peak has been motivated by the desire to locate the nucleus of NGC 1068 and to establish the relation between the radio structure and the emission-line kinematics. Our results show that cloud B is completely resolved at the 0.″05 scale and there is no evidence for an embedded point source. Its morphology is not circular but rather C-shaped or parabolic, and this argues against this region being the true nucleus.

The UV continuum emission peak is shifted 0.″05 toward the north (P.A. -17 ± 11) with respect to the [O III] peak, a result consistent with the optical continuum displacement estimated by Evans et al. (1991). The high polarization (Antonucci et al. 1994) shows that a substantial amount of the emission must be scattered radiation. However, its color is significantly bluer

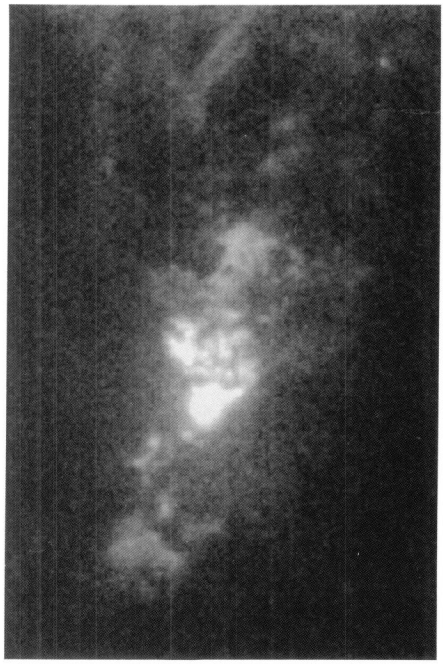

FIG. 1*a*

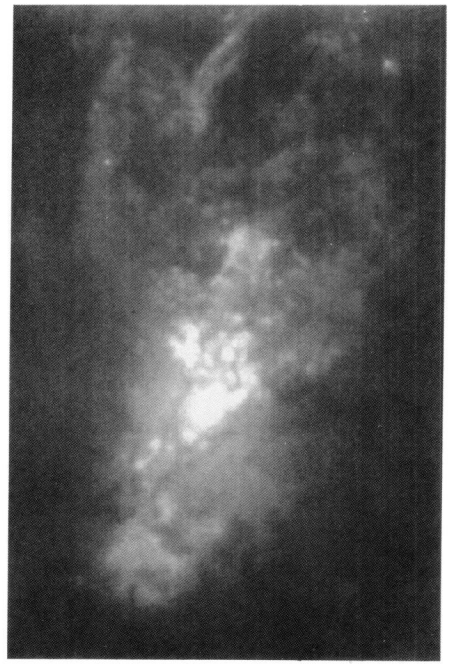

FIG. 1*b*

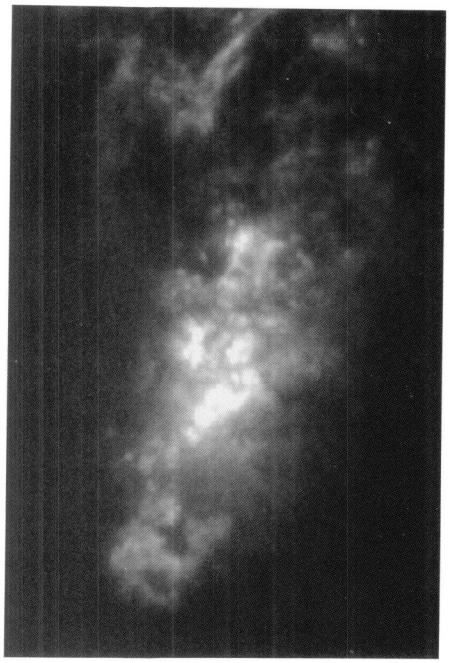

FIG. 1*c*

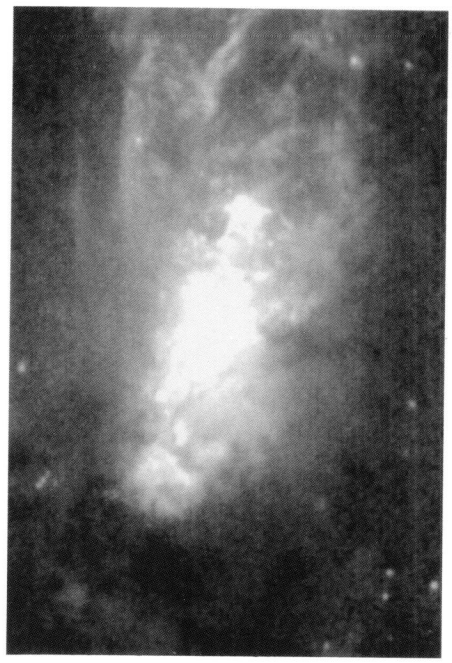

FIG. 1*d*

FIG. 1.—FOC images of NGC 1068 taken with the F253M (*a*), F372M (*b*) and F501N (*c*). The field of view is 4″ × 6″. (*d*) A summed images at higher contrast and large field of view (5″ × 7″). The images are oriented with the *Y*-axis oriented at P.A. +40° from the north.

MACCHETTO et al. (see 435, L16)

FIG. 2.—Composite color image in which the U' is assigned to "red," UV continuum to "blue" and the [O III] line emission image to "green." This rendering is dominated by the differences between the U' continuum and [O III] emission. The field of view is 6″ × 7″.

MACCHETTO et al. (see 435, L16)

PLATE L6

FIG. 3*a*

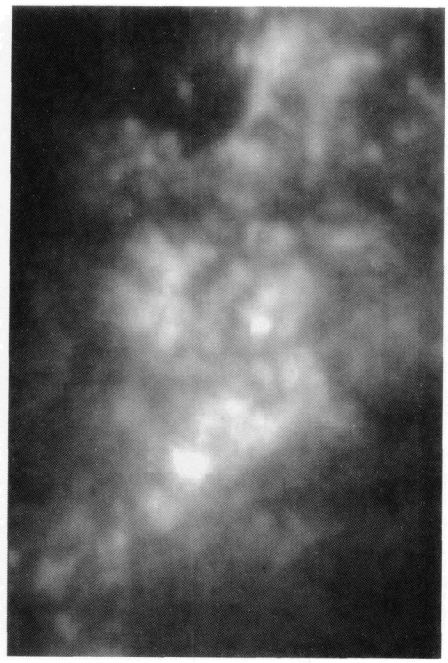

FIG. 3*b*

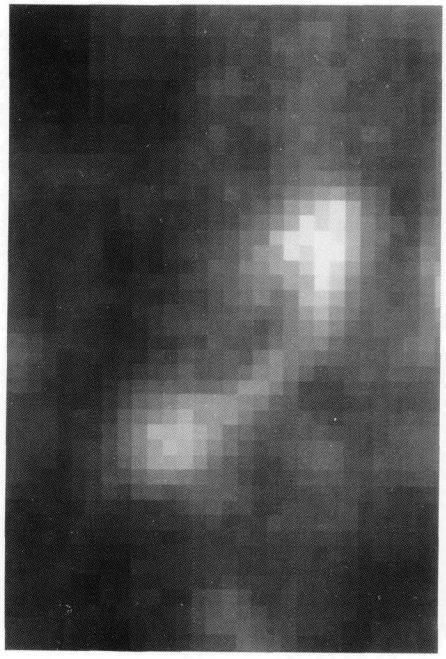

FIG. 3*c*

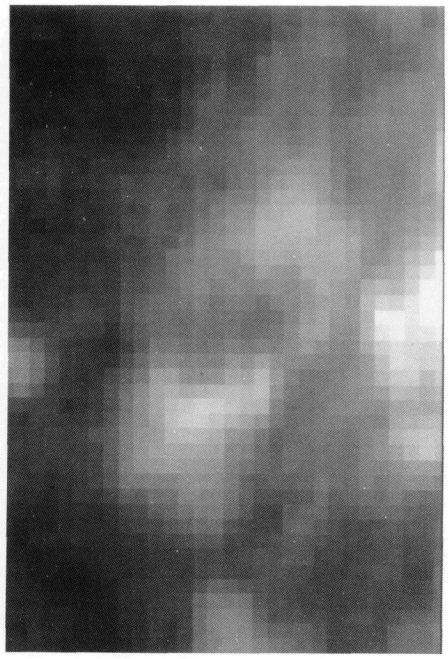

FIG. 3*d*

FIG. 3.—(*a*) and (*b*) Expanded versions of the innermost regions in the UV continuum and emission line, respectively. The field of view is 2″.0 × 2″.5. (*c*)–(*d*) Comparison of the "twin-crescent" structure in the F372M (*c*) and F501N (*d*)

1994ApJ...435L..15M

FIG. 4*a*

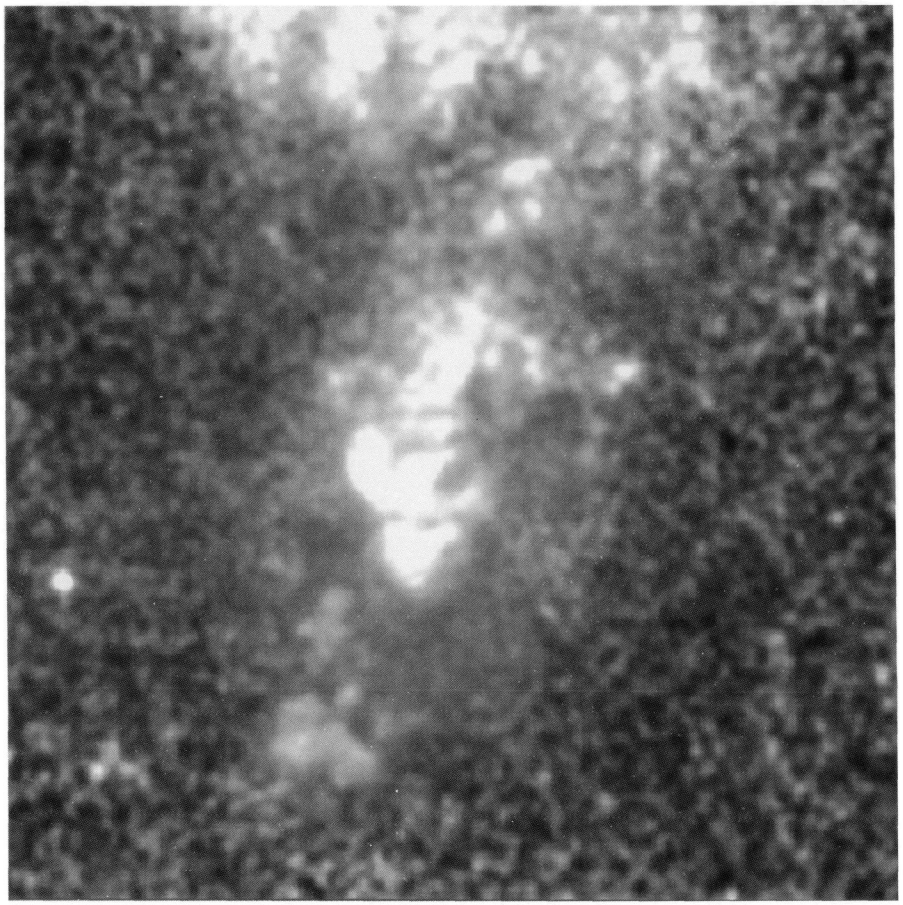

FIG. 4*b*

FIG. 4.—(*a*) Ratio between the UV and U' continuum image; lighter colors correspond to a bluer spectrum. (*b*) Ratio between the U' continuum and emission-line image. The "twin-crescent" structure and cloud B stand out as regions of excess of continuum emission.

than is typical for the rest of the NLR. Three processes may contribute to this result: (1) cloud B is colinear with the inner radio structure and may have a more direct view of the nucleus; (2) there is an intrinsic blue emission component in this region; (3) the scattering medium varies from location to location, with cloud B preferentially scattering the short-wavelength radiation.

The observed displacement between the continuum and emission-line peaks is as expected for fast shock models in which finite cooling lengths are important (Taylor, Dyson, & Axon 1992). Unfortunately, the registration between the radio and optical astrometric reference frames is uncertain to ~0".5, and this interpretation cannot be tested.

3.3. *The "Twin-Crescent" Structure*

An interesting feature is the "*twin-crescent*" structure (Figs. 3*c* and 3*d*). It is extended ~0".4 (~40 pc) in the north-south direction and ~0".1 in the EW direction and oriented at PA +4°. It is asymmetrical in the continuum, with its northern side brighter than the southern; the asymmetry does not depend on the wavelength. Comparison of Figures 3*c* and 3*d* indicates that the line and continuum emission morphology is significantly different.

Both this object and cloud B stand out as regions of excess of blue continuum emission which are not typical of the NLR as a whole. We quantify this in Figure 4*b*, which maps the intensity ratio U' over [O III]. The average value of this flux ratio is 0.05 in the emission-line region, whereas on cloud B it is 0.14 and on the "twin crescent" it is 0.19. Even with its excess blue continuum, this peculiar object is still prominent as an emission-line feature in Figure 3*d*.

Imaging polarization observations by Capetti et al. (1994) have shown that the "twin crescent" is highly polarized (~45%). They also have determined the exact location of the nucleus (within 0".05) by locating the center of symmetry of the polarization pattern. This is 0".6 south of the peak of emission and close to the center of the "twin-crescent" feature, suggesting a physical connection with the nucleus.

It is unlikely that the feature is a disk (or torus) because it is misoriented with respect to the radio lobes and cones. A more plausible interpretation is that the "twin-crescent" may represent an expanding bipolar structure, or jet, similar to that of HH 34, Morse et al. (1992), and as in that case, may be due to bow shocks from material ejecta ploughing through the ISM. Because of the very high level of polarization (~45%; Capetti et al. 1994), an alternative is that it is an echo or reflection of light from the true, hidden nucleus which would lie between the two bright lobes, at least approximately.

3.4. *The Point Sources*

Ten point sources are present in the field of view, nine of which are not visible in the pre-COSTAR observations. None of these are seen in the [O III] image, which excludes the possibility that they are unresolved line-emitting clouds. All of them are bright enough for an estimate of the flux in both the UV and U' images (see Table 1). The two brighter sources are located within the region where we detected reflected nuclear light. However, the brighter source which is seen in the pre-COSTAR observations shows very little polarization (Capetti et al. 1994) indicating that its emission is produced in situ and is not reflected.

The observed colors of these sources are bluer than globular clusters; a single O3 star at the distance of NGC 1068 would be as bright as the weaker point sources, but in contrast would be much bluer. These alternatives can be excluded. It is well known that the inner region of NGC 1068 is a site of active star formation (e.g., Telesco, Becklin, & Wynn-Williams 1984). The colors and luminosities are in good agreement with those of OB associations of a few tens up to 100 stars at the distance of NGC 1068. For example, the brightest source has a specific luminosity of 5×10^{35} ergs s^{-1} Å^{-1}, corresponding to the luminosity of ~100 B0 stars. In addition, a resolved blue object in the field has almost the same color and luminosity, and it is probably also an OB association.

4. SUMMARY AND CONCLUSIONS

We have presented imaging observations of the Seyfert galaxy NGC 1068 taken with the COSTAR-corrected FOC on *HST*, in the UV continuum, optical continuum, and [O III] emission lines. The NLR is seen to possess an extremely complex structure. Globally, there is a now familiar conelike morphology generally attributed to anisotropic illumination from the AGN, but in detail there are subtleties: the axis of symmetry and location of the apex depend upon the intensity level at which the images are presented. The peak of optical and UV continuum emission lie at the same location, but displaced from that of the [O III] line emission peak. The continuum peak is well resolved and shows no sign of a point source within it. It is therefore unlikely to be the true nucleus, consistent with the idea that the true nucleus is completely obscured and hidden from our direct view. New individual features are

TABLE 1

PHOTOMETRY OF THE POINT SOURCES

Offset from the Continuum Peak	F372M (10^{-18} ergs s^{-1} cm^{-2} Å^{-1})	F253M (10^{-18} ergs s^{-1} cm^{-2} Å^{-1})	Color[a] $-2.5 \log (F_{253}/F_{372})$
+1".6, +3".1.....	13.8	14.4	−0.05
−0.9, +2.3.....	9.8	5.6	+0.61
+2.6, −2.4.....	3.1	5.5	−0.62
−2.2, −0.1.....	2.6	5.4	−0.79
+2.1, −2.9.....	2.2	5.8	−1.05
+2.0, −2.5.....	2.2	4.3	−0.73
+2.2, +3.1.....	2.1	2.5	−0.19
+1.3, −1.5.....	1.5	2.7	−0.64
−1.8, −1.3.....	1.1	2.6	−0.93
+2.1, −2.2.....	0.8	2.4	−1.19

[a] With this definition, for a comparison, the color of Vega is +0.13.

identified in these images, including what may be a bipolar jet emerging from the nucleus (the "twin crescent"). Individual blue point sources are also found indicating ongoing star formation in the nuclear regions.

In the future, it would be highly desirable to obtain high-resolution *HST* long-slit spectroscopy and polarimetry in order to allow more detailed models of the NLR to be constructed, and to assess the relationship between gas motions dominated by galactic processes and those influenced by the AGNs.

REFERENCES

Antonucci, R. R. J., & Miller, J. S. 1985, ApJ, 297, 621
Baldwin, J. A., Wilson, A. S., & Whittle, M. 1977, ApJ, 319, 84
Capetti, A., Axon, D., Macchetto, F., Sparks, W. B., & Boksenberg, A. 1994, ApJ, submitted
Cardelli, J. A., Clayton, G. C., & Mathis, J. S. 1989, ApJ, 345, 245
Evans, I. N., Ford, H. C., Kinney, A. L., Antonucci, R. R. J., Armus, L., & Caganoff, S. 1991, ApJ, 369, L27
Hester, J. J. 1994, in preparation
Jedrzejewski, R. J., Hartig, G., Jakobsen, P., Crocker, J. H., & Ford, H. C. 1994, ApJ, 435, L7
Meaburn, J., & Pedlar, A. 1986, A&A, 159, 336
Morse, J. A., Hartigan, P., Cecil, G., Raymond, J. C., & Heathcote, S. 1992, ApJ, 399, 231
Paresce, F. 1992, Faint Object Camera Instrument Handbook Version 3.0 (Baltimore: Space Telescope Science Institute)
Pogge, R. W. 1988, ApJ, 328, 519
Taylor, D., Dyson, J. E., & Axon, D. J. 1992, MNRAS, 255, 351
Telesco, C. M., Becklin, E. E., & Wynn-Williams, G. G. 1984, ApJ, 282, 427
Unger, S. W., Lewis, J. R., Pedlar, A., & Axon, D. J. 1992, MNRAS, 258, 371
Unger, S. W., Pedlar, A., Axon, D. J., Whittle, M., Meurs, E. J. A., & Ward, M. 1987, MNRAS, 228, 671
Wilson, A. S., & Ulvestad, J. S. 1983, ApJ, 275, 8